EPJ Web of Conferences **249**, 07002 (2021) https://doi.org/10.1051/epjconf/202124907002
Powders and Grains 2021

Effect of particle shape on particle breakage inside rotating cylinders

Luisa Fernanda Orozco[1,3], *Jean-Yves* Delenne[2], *Philippe* Sornay[3], and *Farhang* Radjai[1,*]

[1]CNRS, LMGC, University of Montpellier, 163 rue Auguste Broussonnet, F-34095 Montpellier, France
[2]IATE, INRA, CIRAD, Montpellier SupAgro, University of Montpellier, France
[3]CEA, DES, IRESNE, DEC, SA3E, LCU, Cadarache F-13108 Saint-Paul-Lez-Durance, France

Abstract. We study the influence of particle shape on the evolution of particle breakage process taking place inside rotating cylinders. Extensive particle dynamics simulations taking into account the dynamics of the granular flow, particle breakage, and polygonal particle shapes were carried out. We find that the rate of particle breakage is faster in samples composed of initially rounder particles. The analysis of the active flowing layer thickness suggests that for samples composed of rounder particles a relatively lower dilatancy and higher connectivity lead to a less curved free surface profile. As a result, rounder particles rolling down the free surface have a higher mobility and thus higher velocities. In consequence, the faster breakage observed for rounder initial particles is due to the larger particles kinetic energy at the toe of the flow.

1 Introduction

In numerous applications e.g. food engineering, pharmaceutical, mining, bio-fuels manufacture, powder metallurgy, tumbling devices are used to perform several industrial processes such as milling, grinding, drying, granulation [1–3]. Drum rotation implies particle flow and it can also lead to desired or undesired particle fragmentation. Therefore, the continuous evolution of the particle size and shape together with the randomness of the initial particle shape that one can find in nature, render particle breakage inside tumbling devices a complex subject that needs a multiscale detailed analysis.

The rotating drum flow configuration presents a continuous, dense free surface flow. Such conditions make this configuration suitable for studying the rheology of granular flows [4]. Indeed, several research works have focused on the flow characterization [5–8] and some have studied the effect of the particle shape [9–12], but there is few work on the effect of particle breakage during the process [13].

This work focuses on the influence of the initial particle shape on the grinding process taking place inside rotating cylinders. Discrete-element simulations applying the Bonded-cells method were performed in 2D to model the dynamics of particle breakage. To capture the effect of particle shape, several samples composed of regular polygons but increasing number of sides were tested under identical system configurations.

The roundness increases with the number of sides and the particles approach a circular shape. The effect of roundness on particle breakage is not intuitive. Indeed, particle breakage is initiated mainly at vertex-side contacts where high stress concentration is expected, and this should lead to lower probability of particle breakage as the roundness increases. On the other hand, when grinding occurs as a result of dense granular flow, rounder particles exhibit larger mobility and hence more energetic collisions that may enhance particle breakage. The grinding evolution was tracked through specific surface measurements (i.e. sum of the particles perimeters normalized by the total mass).

In the following, the simulation methodology and sample characteristics are introduced. Then, the grinding evolution will be presented and analyzed.

2 Simulation Procedures

Numerical 2D simulations were performed by means of the contact dynamics method together with the Bonded-cell method (BCM) that deals with particle breakage. Contact Dynamics is a discrete-element method in which perfectly rigid particles interact through frictional contacts, and the particle motions are calculated by a step-wise implicit scheme [14–18]. A particularity of Contact Dynamics is that the velocities and contact forces are simultaneously calculated through an iterative process accounting for the contacts as unilateral constraints. From the obtained solution, the contact network and the particles positions are updated.

In the framework of BCM, a Voronoï tessellation is applied to each particle in order to subdivide them into smaller independent elements called *cells*. The average cell size d_{cell} is fixed such that each primary particle has around 20 cells, but the cell shapes are random. As a consequence, the particle volume is exactly equal to the sum of cell volumes [19–23]. In the generated sample, interfaces between adjacent cells belonging to a same particle

*e-mail: franck.radjai@umontpellier.fr
A video is available at https://doi.org/10.48448/h1ht-g784

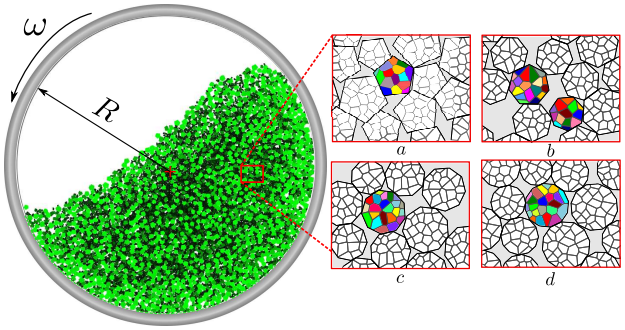

Figure 1. Geometry parameters of the simulated drum in 2D. The colors of the particles are proportional to the damage ranging from bright green for intact particles to black for completely broken fragments. The zoom windows show the initial state of different samples with n_{sides} = a) 5, b) 7, c) 9, and d) 12. Each cell is represented with a different color.

are side-side, and each contact is represented by two cohesive bonds. However, other types of contacts such as vertex-side and vertex-vertex are represented by a single cohesionless contact point. The breakage of a cohesive bond takes into account two criteria: 1) A tensile stress threshold C_n in the normal contact direction and a shear stress threshold C_t in the tangential direction. The relative movement between two cells in contact is forbidden as long as the stress remains below the corresponding threshold. 2) A fracture energy $\mathcal{W}$ that must be consumed by the relative displacements at the stress threshold as in the classical fracture mechanics. Further details about the breakage model can be found in [13].

For the sake of geometric consistency, the external shapes of the particles are polygonal, as the cells. We considered different samples composed of initial particles with a given number of sides n_{sides}; See fig. 1. The sample particle size follows a uniform distribution in particle volumes in a range between d_0^{min} and d_0^{max}. The generated sample is deposited inside a hollow drum (ring in 2D) of internal radius R under the action of gravity g (See Fig. 1). A constant angular velocity $\omega = 3.14$ rad/s is applied to the drum until a full breakage state is achieved (i.e. the fragments size reach d_{cell}). The Froude number Fr= $\omega^2 R/g$, common for all tested systems, has a value of 0.21 and a cascading flow regime is obtained. The values of all parameters considered in this work are presented in Table 1.

Table 1. Simulation parameters

Geometrical parameters		
Number of particles	N_p	[1600;2000]
Number of cells per particle	n_{cells}	[16;36]
Number of cells (total)	N_{cells}	[24000;30000]
Particle density	ρ	2030 kg m^{-3}
Drum internal radius	R	0.075 m
Initial mean particle diameter	$\langle d_0 \rangle$	2.5 mm
Cell size	d_{cell}	$0.5 \cdot 10^{-3}$ mm
Number of sides	n_{sides}	[5,6,7,9,12]
Mechanical parameters		
Friction coefficient	μ	0.4
Normal stress threshold	C_n	1 MPa
Tangential stress threshold	C_t	1 MPa
Fracture energy per length unit	$\mathcal{W}/\ell$	50 J/m
Kinematic parameters		
Rotation speed	ω	5.23 rad/s
Froude number	Fr	0.21
Gravity acceleration	g	9.81 m/s^2

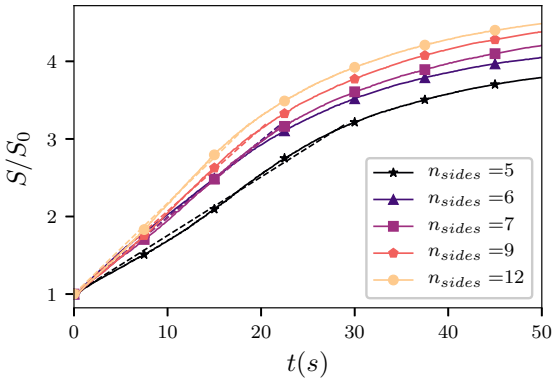

Figure 2. Specific surface S normalized by its initial value S_0 for each sample of polygons with different numbers of sides n_{sides}.

3 Results

3.1 Particle breakage

Since no grinding media (as in ball mills) was considered, particle breakage is a mere consequence of collisions between particles and with the drum walls. The grinding can be characterized through the evolution of specific surface area S, defined as particle surface per unit mass, presented in Fig. 2. The linear-like monotonic evolution reflects the surface generation during particle breakage. Indeed, once a particle is broken the cohesion is not restored, so that nor re-agglomeration neither healing processes are considered in the model. Once a fragment size reach d_{cell}, no further fragments can be generated so that S gradually tends to a *plateau*.

In the linear regime, the specific surface increases all the more faster that the number of sides is larger. This is what we observe more clearly in Fig. 3, in which the grinding rate $\dot{S}/S_0$ is presented as a function of n_{sides}. The grinding rate is the slope of the linear trend presented as dashed lines in Fig. 2.

3.2 Active layer

The active layer or flowing layer is the portion of the granular bed that flows in the opposite direction to the imposed wall velocity (i.e. red portion in Fig. 4). The thickness of the the active layer h_{act} is measured in the velocity profile calculated at the mid-chord length from the free surface in the direction perpendicular to the flow. In Fig. 5 we observe a monotonic increase on the average active layer thickness regarding n_{sides}. This means that for samples

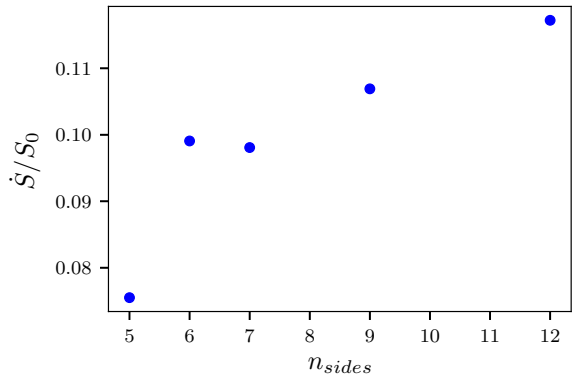

Figure 3. Grinding rate $\dot{S}/S_0$ for samples of polygons with different numbers of sides n_{sides}.

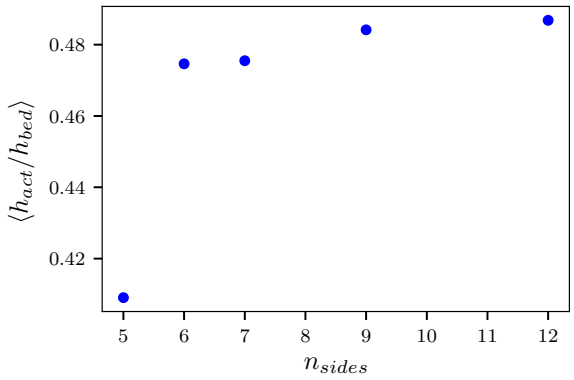

Figure 5. Mean active layer thickness h_{act} normalized by the granular bed thickness h_{bed}, for each sample of breakable polygons with different number of sides (n_{sides}).

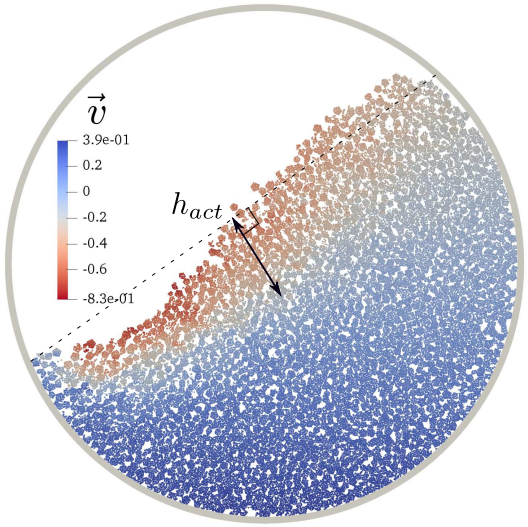

Figure 4. Velocity field (velocity projected in the stream direction $\vec{v}$) of a sample with $n_{sides} = 5$.

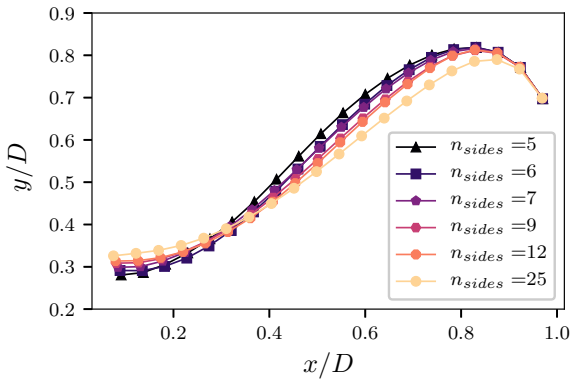

Figure 6. Free surface profiles for each sample of unbreakable polygons with different number of sides (n_{sides}).

composed of rounder particles an increasing amount of particles flow down the slope. This is also a signature of the higher mobility that these samples present as compared to samples composed of more angular particles.

Note that in Figs. 3 and 5 the values for the configurations with $n_{sides} = 6$ increase drastically, so that they are out of the trend followed by the rest of the data. This behavior is due to the long-range correlations enhanced by the regular shape. Such irregularities in the flow are more present in samples with $n_{sides} = 5$ and $n_{sides} = 6$ and they vanish for rounder particles. On the other hand, the samples composed of more angular particles present steeper free surface profiles (e.g. a more pronounced S-shape, see Fig. 6). The microstructure may also play a key role, that we investigate in more detail below.

3.3 Connectivity

The connectivity of particles is linked to several rheological properties such as packing fraction and macroscopic friction coefficient [24]. The coordination number, a typical measurement of the connectivity, is defined as $Z = 2N_c/N_p$, where N_c is the number of interactions and N_p the number of particles. Each interaction involves only two particles, so that Z represents the number of touching neighbors per particle irrespective of the nature (side-side, side-vertex, vertex-vertex) of the contacts. The partial coordination number or connectivity number Z_c is defined in a similar way but by counting each side-side contact as two simple contacts. This is because a line contact is equivalent to two constraints concentrated at two points belonging to that line whereas a vertex-side contact is a point constraint.

Fig. 7 displays the time evolution of Z and Z_c (inset) for samples composed of unbreakable polygons with different values of n_{sides}. We see that samples composed of rounder particles exhibit smaller values of Z, and Z_c shows larger changes as the initial particle shape gets more angular. This means that angular particles are more tightly connected and these samples present lower volume change. This is consistent with the free surface shape for different

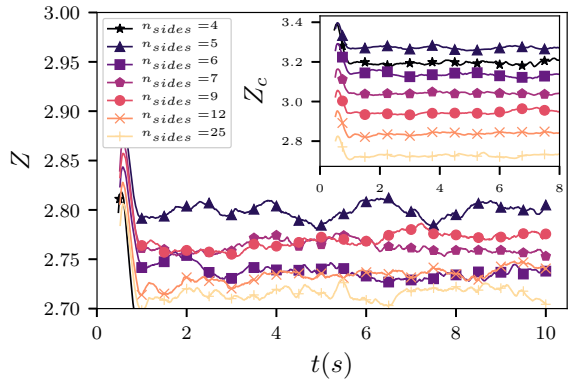

Figure 7. Evolution of the particle connectivity Z and Z_c of non-breakable samples of regular polygons with different shapes.

values of n_{sides} (See Fig. 6), where rounder particles samples present a flatter profile.

The effect of roundness as analyzed here can be compared to the cushioning effect observed in polydisperse flows [25]. Smaller particles in the pores between larger particles lead to a higher coordination number of large particles, and hence a more isotropic distribution of stresses, which reduces their breakage rate. In the case of a rotating drum and during flow, a lower connectivity together with higher mobility leads to higher particle breakage.

4 Discussion and conclusion

In this paper, we studied the effect of the initial roundness of particles on the particle breakage evolution during grinding inside rotating drums. Simulations of breakable samples composed of polygons of different shapes were performed in the framework of DEM coupled with the Bonded-Cell Method. The results show that the initial particle shape plays a role on the grinding rate inside rotating drums. In particular, we found that the grinding occurs faster for samples of rounder initial particles.

The monotonic increment of the active layer thickness with the initial particle roundness means that there is a better mobility for rounder particles down the slope. Due to their higher mobility, rounder particles flow easier leading to higher velocities and higher collision forces. Also, rounder particles are better connected and therefore, a lower sample dilatancy and less steep free surface profiles are exhibited during the flow. These two features (i.e. higher mobility and lower dilatancy) seem thus to be at the origin of larger particle fragmentation inside rotating cylinders.

To sum up, the increasing grinding rate found for samples composed of rounder initial particles can be explained by the fact that rounder particles flow easier down the slope, show lower dilatancy and are better connected. These flow features lead to higher velocities and collision forces at the toe of the flow and thus higher likeliness of particle breakage. These features hold also in 3D and we therefore expect also higher grinding rate in 3D, which needs to be checked either with experiments or 3D simulations.

References

[1] O. Dubé, E. Alizadeh, J. Chaouki, F. Bertrand, Chem Eng Sci **101**, 486 (2013)
[2] R.M. De Carvalho, L.M. Tavares, Miner Eng **43-44**, 91 (2013)
[3] M. Capece, E. Bilgili, R. Davé, Chem Eng Sci **117**, 318 (2014)
[4] G. MiDi, Eur Phys J E **14**, 341 (2004)
[5] A. Alexander, T. Shinbrot, F.J. Muzzio, Powder Technol **126**, 174 (2002)
[6] N. Taberlet, P. Richard, E. John Hinch, Phys Rev E **73**, 1 (2006)
[7] F. Pignatel, C. Asselin, L. Krieger, I.C. Christov, J.M. Ottino, R.M. Lueptow, Phys Rev E **86**, 1 (2012)
[8] L.F. Orozco, J.Y. Delenne, P. Sornay, F. Radjai, J Rheol **64**, 915 (2020)
[9] J. Olson, M. Priester, J. Luo, S. Chopra, R.J. Zieve, Phys Rev E **72**, 1 (2005)
[10] D. Höhner, S. Wirtz, V. Scherer, Powder Technol **253**, 256 (2014)
[11] G. Lu, J.R. Third, C.R. Müller, Particuology **12**, 44 (2014)
[12] N. Gui, X. Yang, J. Tu, S. Jiang, Powder Technol **318**, 248 (2017)
[13] L.F. Orozco, J.Y. Delenne, P. Sornay, F. Radjai, Phys Rev E **101**, 1 (2020)
[14] J.J. Moreau, Eur J Mech A-Solid **13**, 93 (1994)
[15] M. Jean, Comput Method Appl M **177**, 235 (1999)
[16] M. Jean, V. Acary, Y. Monerie, Philos T R Soc S-A **359**, 2497 (2001)
[17] F. Radjai, V. Richefeu, Mech Mater **41**, 715 (2009)
[18] F. Radjai, F. Dubois, *Discrete-element modeling of granular materials* (Wiley-Iste, 2011)
[19] D.H. Nguyen, E. Azéma, P. Sornay, F. Radjai, Phys Rev E **91**, 022203 (2015)
[20] D. Cantor, E. Azéma, P. Sornay, F. Radjai, Comput Particle Mech **4** (2017)
[21] D.H. Nguyen, E. Azéma, P. Sornay, F. Radjai, Eur Phys J E **41**, 50 (2018)
[22] L.F. Orozco, J.Y. Delenne, P. Sornay, F. Radjai, Int J Solids Struct **166**, 47 (2019)
[23] L. Orozco, D. Nguyen, J.Y. Delenne, P. Sornay, F. Radjai, Powder Techno **362**, 157 (2019)
[24] F. Radjai, J.N. Roux, A. Daouadji, J Eng Mech **143**, 04017002 (2017)
[25] O. Tsoungui, D. Vallet, J. Charmet, Powder Technol **105**, 190 (1999)